Supercontinuum generation in water by intense, femtosecond laser pulses under anomalous chromatic dispersion

Parinda Vasa,[1,*] Jayashree A. Dharmadhikari,[2] Aditya K. Dharmadhikari,[3] Rahul Sharma,[1] Mamraj Singh,[1] and Deepak Mathur[2,3,†]

[1]*Department of Physics, Indian Institute of Technology Bombay, Mumbai 400 076, India*

[2]*Centre for Atomic and Molecular Physics, Manipal University, Manipal 576 104, India*

[3]*Tata Institute of Fundamental Research, 1 Homi Bhabha Road, Mumbai 400 005, India*

(Received 14 March 2014; published 21 April 2014)

We report efficient generation of a broadband supercontinuum (SC) in water upon irradiation by intense, near-infrared, femtosecond laser pulses. The SC spectra generated when the pump wavelength lies in the anomalous chromatic dispersion region are characterized by largely blueshifted peaks in the visible range. These SC spectral features are rationalized within the framework of a phenomenological self-phase-modulation model, taking into account higher-order group velocity dispersion. Our model provides an intuitive explanation for the relation between the observed pump-wavelength dependence of the blueshifted SC peaks and the anomalous chromatic dispersion.

DOI: 10.1103/PhysRevA.89.043834 PACS number(s): 42.65.Ky, 42.65.Jx, 42.65.Re

I. INTRODUCTION

The phenomenon of supercontinuum (SC) or white-light generation that accompanies the propagation of intense, short, optical pulses through transparent media can result in significant spectral broadening covering a wide range from the UV to the IR [1,2]. SC generation in various gaseous, liquid, and solid media has been explored and intensively investigated for over the last three decades [3] as it offers opportunities to probe diverse, and fascinating, facets of nonlinear light-matter interactions [4,5]. It is also useful for potential applications involving development of ultrafast lasers [6,7], imaging, and microscopy [8–10]. Considerable work has been reported in recent years on SC generation in condensed media as a function of laser energy, polarization, pulse duration, and focusing conditions. In spite of intense efforts, some basic features of SC generation, particularly those involving the role of higher-order chromatic or group velocity dispersion (GVD), are yet to be fully understood. This is because most of the experimental work has been carried out at pump wavelength $\lambda_{pu} = 800$ nm and under normal conditions of GVD [11–14]. In recent times, groups investigating filamentation and SC generation in solid dielectrics under anomalous dispersion have discovered, both theoretically [15,16] and experimentally [5,7,16,17], the emergence of a greatly blueshifted broad peak in the visible part of the SC spectra. The resulting broad continuum can span more than 3.3 octaves, offering prospects of temporal compression into a single-cycle pulse [6,7,15,16]. The appearance of the blueshifted peak has been attributed either to the interference and self-phase modulation of the SC light field undergoing anomalous GVD [15,16] or via an effective three-wave mixing involving phase matching in which GVD also plays a crucial role [5]. In general, chromatic dispersion is shown to be a key player in determining the spectral extent of the SC spectrum [4,17–20], in addition to other nonlinear processes like self-phase modulation, self-steepening, and intensity clamping. The physical mechanism behind the apparently crucial role that is played by chromatic dispersion remains unclear.

For investigations of SC generation in transparent liquid media, water is a natural choice due to its importance in biological systems as well as its optical properties. Work has been reported on how SC broadening is curtailed when water is doped with small quantities of proteins [21,22] or enhanced by doping it with metal nanoparticles [23]. Filamentation in water doped with DNA plasmids has also been utilized to experimentally probe single and double strands breaks under near-physiological conditions [24,25]. As already noted, almost all such studies, both basic and applied, have been conducted in the normal-dispersion regime. Even though theoretical modeling has shown that anomalous GVD can drastically alter the SC spectrum of water, there continues to be a paucity of work reported in this regime. We know of only two experimental reports on SC generation in the anomalous GVD regime in water, one using 1055 nm, 1 ps pulses in a 3-cm-long cell [18] and the other using 1200 nm, 45 fs pulses in a water-filled photonic crystal fiber [26]. We report in the following results of a systematic experimental study in which we measure the spectral extent of the SC using incident wavelengths in the IR region so as to access different GVD regimes in water. We observe that, in spite of high absorption in water at wavelengths greater than 1300 nm, more than two octaves of spectral broadening is readily obtained. With the help of a phenomenological self-phase-modulation model we provide an intuitive rationalization for the dependence of the SC spectral features on the anomalous chromatic dispersion. We also demonstrate relatively flat and enhanced SC generation in water that is doped with metal nanoparticles under anomalous GVD.

II. EXPERIMENTAL METHOD

Our SC and filamentation experiments were performed using an amplified Ti:sapphire laser system (OdinII) that generated ~35 fs pulses centered at 805 nm with a repetition

*parinda@iitb.ac.in
†atmol1@tifr.res.in

 ©2014 American Physical Society

rate of 1 kHz. These pulses pumped an optical parametric amplifier (OPA) that was tunable over the wavelength range 1200–2400 nm. The OPA's pulse duration, measured using a homemade autocorrelator, was typically 55 fs at 1300 nm. The spectral extent $\Delta\lambda$ of the pulses (defined as the full width at 10% of the maximum intensity) was typically 58 nm at 800 nm and 115 nm over the range 1200–1350 nm. These pulses were focused within a 1-cm-long fused silica cuvette by a lens of 10 cm focal length to a beam diameter of $\sim$10 μm. The beam was focused close to the center of the cuvette to avoid any SC contribution from the cuvette walls. Typical peak power values used in our experiments were P_{pu} = 55–110 MW, corresponding to peak intensities in the range of $\sim 10^{14}$ W/cm^2. These peak powers were sufficient to generate a stable single filament but were moderate enough to preclude formation of multiple filaments. Single-filament generation was confirmed by visual determination of the threshold for SC generation and by inspection of the transmitted SC spot in the far field [27].

The spatially integrated SC spectra generated were spectrally characterized in transmission using either an Ocean Optics visible USB4000 spectrometer (wavelength range 350–1040 nm) or an Aventes IR spectrometer (wavelength range 1000–2500 nm). We calibrated both spectrometers using a standard calibration lamp source (Ocean Optics) so that spectral irradiance could be determined. The aqueous gold colloid used in our experiments contained monodispersed gold nanorods (Nanopartz Inc., USA) in distilled water, with a residual surfactant concentration of $<$100 mM. A typical linear extinction spectrum of our gold-nanorod-doped water and some electron microscope images of the nanorods are shown in the Appendix. The colloid exhibited prominent extinction peaks due to scattering induced by surface plasmon resonance (SPR) [23,28], at 626 nm (characteristic of nanorods with diameter d = 30 nm and length l = 60 nm). The typical filling factor was $\sim 10^{-6}$. Such a low filling factor is necessary to maintain interparticle separation of $\sim$2 μm to avoid any interparticle interactions.

III. RESULTS AND DISCUSSION

A. Supercontinuum spectra

A typical spectral extent of the SC we generated in undoped water (without nanorods) by pump pulses centered at λ_{pu} = 1300 nm and P_{pu} = 90 MW is shown in Fig. 1. Water exhibits appreciable absorption (2.5 cm^{-1}) at this wavelength and, hence, we access the anomalous-dispersion regime in these experiments. We obtain unexpectedly broad SC spectra, with the spectral extent ranging from 350 to 1750 nm, exceeding two octaves. We estimate the SC generation efficiency to be as high as 6%. The SC spectrum is characterized by a largely blueshifted peak at 480 nm. We also note a prominent dip appearing near 760 nm [5,15], between the blueshifted peak and λ_{pu}. The SC spectrum generated at λ_{pu} = 1350 nm and P_{pu} = 500 MW is also shown for comparison. Much higher pulse energy than that required to generate a single filament is used to get a SC spectral strength that is similar to that generated by λ_{pu} = 1300 nm. Due to its higher absorption (5 cm^{-1}), the SC generation efficiency is now

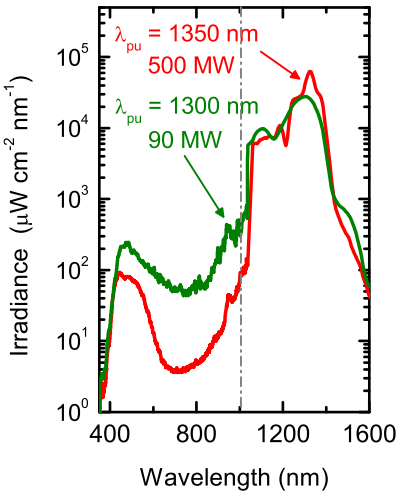

FIG. 1. (Color online) Supercontinuum (SC) spectra generated in undoped water by 55 fs pulses at λ_{pu} = 1300 nm (P_{pu} = 90 MW, green) and λ_{pu} = 1350 nm (P_{pu} = 500 MW, red). Even though both the pump wavelengths are within the anomalous chromatic dispersion range (appreciable absorption) of water, the SC spectra are surprisingly broad, spanning more than two octaves. They are characterized by well-separated peaks in the visible range. Note the blueshift and the narrowing of the visible peak with increasing λ_{pu}.

reduced to 3% even at such high power but the SC continues to extend over more than two octaves (350–1750 nm). The blueshifted peak is now observed to appear at 450 nm; it is significantly narrower than that obtained with λ_{pu} = 1300 nm. The SC spectrum is seen to have a prominent dip at 710 nm.

Similar peaks have been predicted in water (and observed in the case of fused silica) in the visible range; these are separated by a region of very weak emission and exhibit narrowing and blueshifting with respect to λ_{pu} under anomalous chromatic dispersion. However, the mechanism that governs the observed dependence on dispersion is not known [4,5,18,29,30]. It is of interest to note that emission of blueshifted wavelengths in the normal-dispersion regime has also been observed and theoretically analyzed in optical fibers when pumped under the anomalous dispersive regime [31–34]. This process is known as emission of Cherenkov radiation (or dispersion waves) and is governed by propagation of solitonlike pulses in the presence of third- and higher-order dispersion. Emission of dispersive waves in nonlinear fiber optics is not limited to pulses propagating in the anomalous-dispersion regime. It has also been numerically and experimentally demonstrated that in optical fibers, even pulses propagating in the normal-dispersion regime in the presence of Raman gain can efficiently excite resonant dispersive radiation [35]. The mechanism behind the emission of Cherenkov radiation has been suggested to be a phase-matching condition between the incident and emitted wavelengths [31–35].

To investigate the changes in the SC spectrum under the presence and absence of anomalous GVD, we have systematically varied the value of λ_{pu} over the range 800–1350 nm. Typical single-filament SC spectra observed in our experiments are

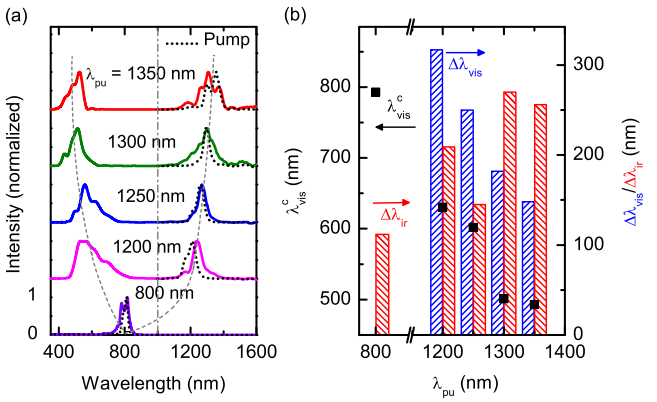

FIG. 2. (Color online) (a) Normalized SC spectra generated in undoped water by femtosecond pulses centered at $\lambda_{pu} = 800$ nm ($P_{pu} = 55$ MW, violet), 1200 nm ($P_{pu} = 55$ MW, magenta), 1250 nm ($P_{pu} = 55$ MW, blue), 1300 nm ($P_{pu} = 55$ MW, green), and 1350 nm ($P_{pu} = 90$ MW, red). Vertical dash-dotted line marks the spectral ranges of the two spectrometers used. The two spectral ranges are normalized separately and spectra are shifted vertically for clarity. Gray dashed lines mark the shift in the SC peaks with λ_{pu}. Pump pulse spectrum (black dotted lines) for each case is also shown for comparison. (b) Spectral position of the visible peak (λ^c_{vis}, symbol) and IR ($\Delta\lambda_{ir}$, red) as well as visible ($\Delta\lambda_{vis}$, blue) spectral extents of the SC as a function of λ_{pu}. Blueshifted peak is seen only when pumped under the anomalous GVD range (>1100 nm). As in Fig. 1, the visible peaks shift to blue and get narrower with increasing λ_{pu}.

shown in Fig. 2. The spectra are corrected for the wavelength-dependent spectrometer response. The GVD changes sign in water at 1100 nm; hence $\lambda_{pu} > 1100$ nm corresponds to pumping under anomalous chromatic dispersion. In this range the spectra exhibit prominent peaks in the IR as well as the visible range, with the visible peak being much weaker (see Fig. 1). In order to better appreciate the spectral features as well as to estimate the spectral extent, we individually normalize the SC spectra in the IR and visible regimes [Fig. 2(a)]. The most striking feature of the normalized SC spectra is a relatively broad and greatly blueshifted peak in the visible region for $\lambda_{pu} > 1100$ nm. Similar blueshifted peaks have been observed in fused silica by Durand *et al.* (Fig. 2 in [5]) It has a significant spectral extent of >100 nm and plays a crucial role in generating the spectrum spanning over more than two octaves. The peak is well separated from λ_{pu} and shifts towards the blue with increasing λ_{pu} [see Fig. 2(b)], ruling out contributions from third-harmonic generation [5]. Its extent is also seen to be reduced [see Fig. 2(b)] as the value of λ_{pu} increases [19]. Considering the absorption in water at near-IR wavelengths, there is also significant broadening near the λ_{pu} value, becoming more prominent in the cases of $\lambda_{pu} = 1300$ and 1350 nm.

B. Modeling SC generation

In order to rationalize our observations of SC generation in undoped water under anomalous chromatic dispersion, we adopt a phenomenological approach. We take the primary origin of SC generation to be self-phase modulation (SPM), which is mainly a third-order nonlinear process governed by the real part of the third-order susceptibility $\chi^{(3)}$ [36–38]. In water, the two main factors [39] that contribute to $\chi^{(3)}$ are (i) laser-induced distortion of the electronic charge distribution (the Kerr nonlinearity) $\chi^{(3)}_{el} = 2 \times 10^{-14}$ esu [40], and (ii) the free-electron- or plasma-induced susceptibility ($\chi^{(3)}_{pl}$). Under our experimental conditions, $\chi^{(3)}_{pl} \sim 10^{-13}$ esu and hence SC generation in water is mainly governed by plasma generation. As a first-order approximation, we assume an instantaneous material response and no significant changes in the pulse profile as it propagates or self-focusing. Under such conditions, the induced time-dependent frequency modulation $\Delta\omega(t) \propto \chi^{(3)} \frac{\partial |E|^2}{\partial t}$, where E is the amplitude of the electric field of a pulse. The generated SC spectrum is then obtained by Fourier-transforming the resultant electric field [37,38]. Therefore the key to understanding SC generation is to probe how the induced phase $\varphi(t)$ or, in turn, the electric-field envelope, evolves with time under anomalous GVD.

The linear optical response of water is shown in Fig. 3(a). The refractive index n is calculated using the Sellmeier equation [41,42] whereas absorbance is a quantity that is measured by us. Water is transparent up to ~1000 nm. At

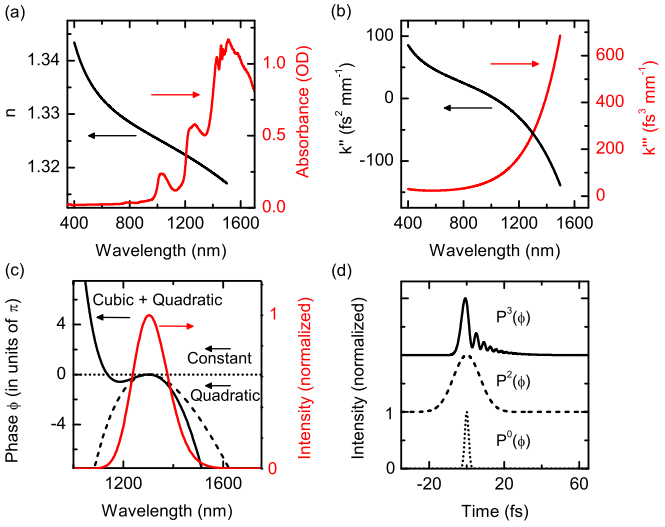

FIG. 3. (Color online) (a) Refractive index (n, black) and measured absorbance (red) in undoped water. The refractive index is calculated using the Sellmeier equation given in the literature [41,42]. (b) Second- (k'') and third- (k''') order GVD coefficients calculated using n shown in (a). The GVD in water changes sign at ~1100 nm. For longer wavelengths, the anomalous chromatic regime is characterized by rapidly increasing k''' due to increasing absorbance. (c) Normalized intensity spectrum (red) of a Gaussian pulse centered at 1300 nm, having FWHM of 100 nm, and its spectral phase in the presence of (i) no dispersion (black dotted), (ii) only second-order GVD (quadratic, black dashed), and (iii) second- and third-order GVD (quadratic + cubic, black solid). (d) Normalized temporal intensity profiles of the Gaussian pulse shown in (c) considering GVD of different orders. $P^n(\phi)$ represents the order of the spectral phase polynomial used to obtain the intensity profile. The temporal profiles are shifted vertically for clarity.

longer wavelengths, the absorption increases rapidly, resulting in anomalous as well as higher-order dispersion. Calculated second- (k'') and third- (k''') order GVD coefficients are shown in Fig. 3(b). We see that there is a significant increase in k''' in the wavelength range 1200–1350 nm. Effects of k'' and k''' on the spectral phase and the intensity envelope of a Gaussian pulse centered at 1300 nm after traveling through water for 0.5 cm are shown in Figs. 3(c) and 3(d), respectively. The second-order GVD broadens the pulse while retaining its temporal profile whereas the third-order GVD totally alters it, resulting in a series of pulses over a much longer duration. Since in SPM the phase follows the intensity profile, $\varphi(t)$ will also exhibit series of rapidly varying modulations on the lagging edge. Such modulations, when Fourier transformed, give rise to a blueshifted peak in the frequency or wavelength spectrum. As seen Fig. 3(d), there are several instants of time when the rate of intensity change is the same, resulting in identical $\frac{\partial\varphi(t)}{\partial t}$ or identical frequency generation with time delay. These frequency components can interfere destructively, resulting in a dip in the SC spectrum [38].

Thus, the separation of the blueshifted peak from λ_{pu} depends on the modulation frequency, higher frequency (larger k''') resulting in larger blueshift. Similar explanations based on the modulated phase and destructive interference have also been given to explain the SC spectra generated in fused silica. The extent of the blueshifted peak varies inversely with the pulse elongation (larger k'' and k'''), again being reduced with increasing λ_{pu}. Along with SPM, pulse propagation through a nonlinear medium also experiences intensity clamping and self-steepening, which also contribute in determining the SC spectrum [4,15]. The spectral extent of the incident pulse [Fig. 2(a)] is relatively narrow for the GVD effects to show up over a propagation of ∼0.5 cm through water. However, in the presence of SPM, there is a considerable amount of spectral broadening around λ_{pu}, enhancing the effect of the GVD by many times as the pulse propagates through water. Apart from the temporal modulations, phase-matching conditions under anomalous dispersion also play a major role in determining the spatial and angular spectral intensity distribution. Experiments have been carried out to demonstrate X-wave and O-wave generation in water [5,18]. Similar phase-matching conditions in the presence of anomalous dispersion have been shown to play a crucial role in the emission of Cherenkov radiation in optical fibers [31–34]. The spectra presented here are spatially integrated and, therefore, our simple model excludes the effects of spatial dispersion and phase matching.

C. Comparison of modeled and measured SC spectra

We have made a comparison of the simulated SC spectra generated by λ_{pu} obtained using the model discussed above and those that are observed, and the results are shown in Fig. 4(a). The simulated spectra also take into account the wavelength-dependent absorption in water. The characteristic features of SC spectra in the presence and absence of the anomalous GVD are seen to be well captured by our model. Even though it is very simple, our model provides an intuitive explanation for the underlying mechanism for (i) the SPM being affected by chromatic dispersion, and (ii) the resulting changes in the SC spectra. To clearly show the effect of individual GVD order, we simulate the spectra considering frequency-dependent phase terms up to fifth order [Fig. 4(b)]. Our simulations reveal that the odd-order terms, the third being the lowest, are essential for the generation of the blueshifted peak. Even-order terms result only in pulse broadening and, hence, can mainly give rise to broadening that is close to λ_{pu}. Since higher-order GVD terms are appreciable in water only under anomalous dispersion conditions, it is necessary to choose $\lambda_{pu} > 1100$ nm to observe these features. Including higher-order terms, up to fifth order, improves the match between our experiments and simulation. Filamentation and SC generation are complex nonlinear processes and may involve contributions from other nonlinear processes, like Raman scattering. Therefore to get an exact match between simulated and observed spectra is expected to be difficult even with more advanced approaches, such as solving the nonlinear Schrödinger equation [4,5,15,43].

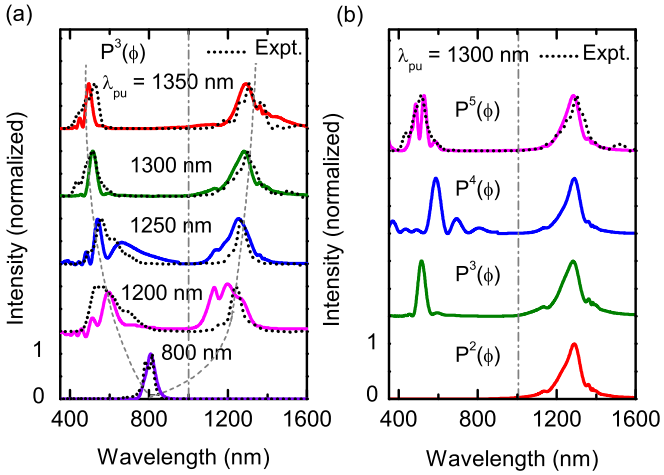

FIG. 4. (Color online) (a) Comparison between the observed (dotted) and simulated (solid) SC spectra after accounting for absorption in undoped water. Vertical dash-dotted line marks the spectral ranges of the two spectrometers used. The two spectral ranges are normalized separately and the spectra are shifted vertically for clarity. Gray dashed lines mark the shift in the SC peaks with λ_{pu}. The SC spectra are simulated using a phenomenological SPM model considering second- and third-order GVD. (b) Effect of various GVD terms on the SC spectrum ($\lambda_{pu} = 1300$ nm). Odd-order GVD (third being the lowest) is essential for the occurrence of the blueshifted peak. Adding higher-order GVD terms to the spectral phase polynomial $P^n(\phi)$ improves the match between simulated and observed spectra.

D. Modifying the SC spectra

So far, we have considered the effect of only the real part of $\chi^{(3)}$. However, at higher peak powers there can be additional nonlinear absorptive processes that contribute to the imaginary part of the nonlinear susceptibility [44]. To understand the effect of intensity-dependent absorption on SC generation, we investigated the SC spectra in water at a higher peak power ($P_{pu} = 110$ MW). A comparison between the SC for two pump wavelengths made in Fig. 5(a) reveals marginal

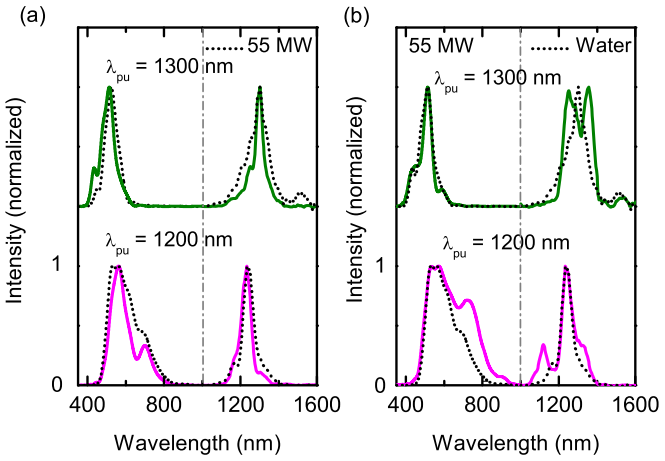

FIG. 5. (Color online) (a) Comparison of normalized undoped-water SC spectra recorded at $P_{pu} \sim 110$ MW (solid) and $P_{pu} \sim 55$ MW (dotted) for $\lambda_{pu} = 1200$ nm (bottom) and $\lambda_{pu} = 1300$ nm (top). There is marginal narrowing of the IR as well as the visible component at higher pump power, possibly due to the competing nonlinear absorptive processes. (b) Enhancement in SC spectral extent by adding metal nanorods to water shown for two pump wavelengths $\lambda_{pu} = 1200$ nm (bottom) and $\lambda_{pu} = 1300$ nm (top) at $P_{pu} \sim 55$ MW. SC spectra for undoped water (dotted) are shown for comparison. Vertical dash-dotted line marks the spectral ranges of the two spectrometers used. The two spectral ranges are normalized separately and spectra are shifted vertically for clarity.

narrowing of the IR as well as the visible component. Similar narrowing, observed earlier for $\lambda_{pu} = 800$ nm, was attributed to the competing imaginary component of $\chi^{(3)}_{pl}$ [23]. We have also observed enhanced SC generation in water doped with gold nanorods that exhibit a SPR at 626 nm [Fig. 5(b)]. The enhancement that is observed is distinctly more prominent at $\lambda_{pu} = 1200$ nm and in the visible range. It is possibly caused by an SPR-induced localization [23,45–47] of the optical field that is experienced by water molecules in the proximity of the nanorods. Spectral overlap of the SPR with the blueshifted peak and the two-photon transition at $\lambda_{pu} = 1200$ nm could have led to the prominent enhancement at this pump wavelength. Also the spectral extent at longer pump wavelength could be limited by the SPR-enhanced absorptive processes. Since the resonance wavelength is very far from the λ_{pu} and the particle concentration is very low, the changes in GVD in the IR range due to the doping are expected to be negligible in such instances.

The results that we have presented here demonstrate that it is possible to exploit (i) the anomalous GVD in water, and (ii) SPR-induced field enhancement in order to produce spectrally flat and broad SC in water at incident values of pulse energy that may be as low as a few microjoules. The resulting SC spectra may be amenable for use in generating single-cycle optical pulses [6,7]. It would, therefore, be of interest to investigate the actual spatiotemporal structure of the emitted field so that suitable compression schemes can be designed and implemented. It would also be interesting to investigate the effect of anomalous dispersion on SC generation in real time, by performing time-resolved experiments.

IV. SUMMARY

In summary, we have investigated the SC generation in water by intense, femtosecond, laser pulses under anomalous chromatic dispersion. Our results show that efficient and broad SC generation in water is possible in spite of the presence of absorption by choosing a pump wavelength longer than 1100 nm. We also show, phenomenologically, that the odd-order GVD plays a crucial role in extending SC in the visible regime. We anticipate that gaining proper insights into the role that GVD plays in SC generation will be useful for developing practical schemes for producing flat and ultrabroad spectra which will be amenable to temporal compression into single-cycle pulses.

ACKNOWLEDGMENTS

Skillful assistance by Rodney Bernard (TIFR) in some stages of the work reported here and helpful discussions with B. P. Singh (IITB) are gratefully acknowledged. We also acknowledge financial support to P.V. from the Industrial Research and Consultancy Centre, IITB (Project No. 12IRCCSG001). We thank the Department of Science and Technology for support to J.A.D. under the Women Scientists Scheme and through the J. C. Bose National Fellowship to D.M.

APPENDIX

We have carried out spectroscopic and structural characterization of gold-nanorod-doped water, and our results are depicted in Fig. 6.

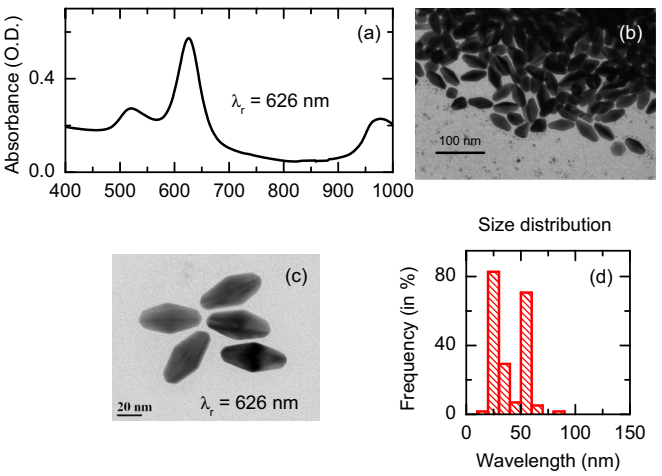

FIG. 6. (Color online) (a) Linear extinction spectrum of the gold-nanorod-doped water showing prominent longitudinal SPR peak at 626 nm and transverse SPR peak at 515 nm. (b),(c) Transmission electron microscope images of gold nanorods (25 nm diameter, 55 nm length) used in our experiments. (d) Size distribution deduced from (b).

[1] A. Couairon and A. Mysyrowicz, Phys. Rep. **441**, 47 (2007).

[2] S. L. Chin, S. A. Hosseini, W. Liu, Q. Luo, F. Théberge, N. Aközbek, A. Becker, V. P. Kandidov, O. G. Kosareva, and H. Schroeder, Can. J. Phys. **83**, 863 (2005).

[3] R. L. Fork, C. V. Shank, C. Hirlimann, R. Yen, and W. J. Tomlinson, Opt. Lett. **8**, 1 (1983).

[4] M. Kolesik, E. M. Wright, and J. V. Moloney, Phys. Rev. Lett. **92**, 253901 (2004).

[5] M. Durand, K. Lim, V. Jukna, E. McKee, M. Baudelet, A. Houard, M. Richardson, A. Mysyrowicz, and A. Couairon, Phys. Rev. A **87**, 043820 (2013).

[6] P. Panagiotopoulos, D. G. Papazoglou, A. Couairon, and S. Tzortzakis, Nat. Commun. **4**, 2622 (2013).

[7] F. Silva, D. R. Austin, A. Thai, M. Baudisch, M. Hemmer, D. Faccio, A. Couairon, and J. Biegert, Nat. Commun. **3**, 807 (2012).

[8] W. Liu, S. Petit, A. Becker, N. Akozbek, C. M. Bowden, and S. L. Chin, Opt. Commun. **202**, 189 (2002).

[9] C. Rewitz, T. Keitzl, P. Tuchscherer, J. S. Huang, P. Geisler, G. Razinskas, B. Hecht, and T. Brixner, Nano Lett. **12**, 45 (2012).

[10] K. Lindfors, T. Kalkbrenner, P. Stoller, and V. Sandoghdar, Phys. Rev. Lett. **93**, 037401 (2004).

[11] A. K. Dharmadhikari, F. A. Rajgara, and D. Mathur, Appl. Phys. B: Lasers Opt. **80**, 61 (2005).

[12] N. T. Nguyen, A. Saliminia, W. Liu, S. L. Chin, and R. Vallée, Opt. Lett. **28**, 1591 (2003).

[13] A. K. Dharmadhikari, F. A. Rajgara, and D. Mathur, Appl. Phys. B: Lasers Opt. **82**, 575 (2006).

[14] H. Dachraoui, C. Oberer, M. Michelswirth, and U. Heinzmann, Phys. Rev. A **82**, 043820 (2010).

[15] E. O. Smetanina, V. O. Kompanets, S. V. Chekalin, A. E. Dormidonov, and V. P. Kandidov, Opt. Lett. **38**, 16 (2013).

[16] E. O. Smetanina, V. O. Kompanets, S. V. Chekalin, and V. P. Kandidov, Quantum Electron. **42**, 920 (2012).

[17] D. Faccio, A. Averchi, A. Lotti, M. Kolesik, J. V. Moloney, A. Couairon and P. Di Trapani, Phys. Rev. A **78**, 033825 (2008).

[18] M. A. Porras, A. Dubietis, E. Kucinskas, F. Bragheri, V. Degiorgio, A. Couairon, D. Faccio, and P. D. Trapani, Opt. Lett. **30**, 3398 (2005).

[19] M. Kolesik, G. Katona, J. V. Moloney, and E. M. Wright, Phys. Rev. Lett. **91**, 043905 (2003).

[20] D. Faccio, A. Averchi, A. Couairon, A. Dubietis, R. Piskarskas, A. Matijosius, F. Bragheri, M. A. Porras, A. Piskarskas, and P. Di Trapani, Phys. Rev. E **74**, 047603 (2006).

[21] C. Santhosh, A. K. Dharmadhikari, K. Alti, J. A. Dharmadhikari, and D. Mathur, J. Biomed. Opt. **12**, 020510 (2007).

[22] C. Santhosh, A. K. Dharmadhikari, J. A. Dharmadhikari, K. Alti, and D. Mathur, Appl. Phys. B: Lasers Opt. **99**, 427 (2010).

[23] P. Vasa, M. Singh, R. Bernard, A. K. Dharmadhikari, J. A. Dharmadhikari, and D. Mathur, Appl. Phys. Lett. **103**, 111109 (2013).

[24] J. S. D'Souza, J. A. Dharmadhikari, A. K. Dharmadhikari, B. J. Rao, and D. Mathur, Phys. Rev. Lett. **106**, 118101 (2011).

[25] A. K. Dharmadhikari, H. Bharambe, J. A. Dharmadhikari, J. S. D'Souza, and D. Mathur, Phys. Rev. Lett. **112**, 138105 (2014).

[26] J. Bethge, A. Husakou, F. Mitschke, F. Noack, U. Griebner, G. Steinmeyer, and J. Herrmann, Opt. Express **18**, 6230 (2010).

[27] A. K. Dharmadhikari, J. A. Dharmadhikari, and D. Mathur, Appl. Phys. B: Lasers Opt. **94**, 259 (2009).

[28] P. K. Jain, K. S. Lee, I. H. El-Sayed, and M. A. El-Sayed, J. Phys. Chem. B **110**, 7238 (2006).

[29] A. Saliminia, S. L. Chin, and R. Vallée, Opt. Express **13**, 5731 (2005).

[30] M. L. Naudeau, R. J. Law, T. S. Luk, T. R. Nelson, and S. M. Cameron, Opt. Express **14**, 6194 (2006).

[31] N. Akhmediev and M. Karlsson, Phys. Rev. A **51**, 2602 (1995).

[32] J. M. Dudley, G. Genty, and S. Coen, Rev. Mod. Phys. **78**, 1135 (2006).

[33] M. Erkintalo, Y. Q. Xu, S. G. Murdoch, J. M. Dudley, and G. Genty, Phys. Rev. Lett. **109**, 223904 (2012).

[34] T. Roger, D. Majus, G. Tamosauskas, P. Panagiotopoulos, M. Kolesik, G. Genty, A. Dubietis, and D. Faccio, arXiv:1404.0937v1.

[35] K. E. Webb, Y. Q. Xu, M. Erkintalo, and S. G. Murdoch, Opt. Lett. **38**, 151 (2013).

[36] Y. R. Shen, *The Principles of Nonlinear Optics* (Wiley, New York, 1984), Chaps. 1, 17, 27, and 28.

[37] R. W. Boyd, *Nonlinear Optics*, 3rd ed. (Academic Press, London, 2008), Chap. 13.

[38] R. R. Alfano, *The Supercontinuum Laser Source*, 2nd ed. (Springer, Heidelberg, 2006), Chap. 1.

[39] M. Kolesik, G. Katona, J. V. Moloney, and E. M. Wright, Appl. Phys. B: Lasers Opt. **77**, 185 (2003).

[40] R. W. Boyd and G. L. Fischer, *Encyclopedia of Materials: Science and Technology* (Elsevier, Amsterdam, 2001), p. 6237.

[41] S. Kedenburg, M. Vieweg, T. Gissibl, and H. Giessen, Opt. Express **2**, 1588 (2012).

[42] Y. Coello, B. Xu, T. L. Miller, V. V. Lozovoy, and M. Dantus, Appl. Opt. **46**, 8394 (2007).

[43] M. Kolesik, J. V. Moloney, and M. Mlejnek, Phys. Rev. Lett. **89**, 283902 (2002).

[44] P. Kaw, G. Schmidt, and T. Wilcox, Phys. Fluids **16**, 1522 (1973).

[45] A. Bouhelier, M. Beversluis, A. Hartschuh, and L. Novotny, Phys. Rev. Lett. **90**, 013903 (2003).

[46] P. Mühlschlegel, H.-J. Eisler, J. F. Martin, B. Hecht, and D. W. Pohl, Science **308**, 1607 (2005).

[47] E. M. Kim, S. S. Elovikov, T. V. Murzina, A. A. Nikulin, O. A. Aktsipetrov, M. A. Bader, and G. Marowsky, Phys. Rev. Lett. **95**, 227402 (2005).